Original Paper

Grazing incidence X-ray reflectivity – a Round Robin test

Report of the International Commission on Glass (ICG) Technical Committee 19 "Glass Surface Diagnostics"

Olaf Anderson and Klaus Bange
SCHOTT GLAS, Mainz (Germany)

Bruno Germain and Patrice Lehuédé
Saint-Gobain Recherche, Aubervilliers (France)

Mark Farnworth
Pilkington Technology, Ormskirk (UK)

Densities and thicknesses of films of five different layer systems were determined in a grazing incidence X-ray analysis (GIXA) Round Robin test carried out by three industrial laboratories. The influence of both the experimental setup and the simulation software on these results is compared for the identical set of samples. Two approaches are adopted; firstly each laboratory measuring and simulating its own data and secondly each laboratory simulating the data that had been measured by another laboratory. The measured data from the three laboratories are analyzed and reasons proposed to explain the relatively minor differences between them. Comparisons are also made between the simulations produced from the two approaches to determine variations and any systematic bias between the three laboratories. Overall, good agreement in film densities and film thicknesses is found, demonstrating the high levels of accuracy that can be obtained from coating analysis using the GIXA technique.

1. Introduction

GIXA (grazing incidence X-ray analysis) or, alternatively, GIXR (grazing incidence X-ray reflectivity) is a very precise method for thickness measurements of layers in the range of 1 to 250 nm. In addition, the determination of density and roughness of layers and substrate can be achieved as well. The need for a perfectly flat sample is a very strong restriction to this technique, however, float glass is generally flat enough to be studied by GIXR. Its main advantage over other experimental techniques is that it may be used to examine the buried interfaces of any number of layers, including the layer with the substrate, without extensive preparation efforts, i.e. thickness and interface roughness and the density for a single film or film systems can be determined.

Film density, film thickness and surface and interface roughness are important quantities, which influence various film properties and last but not least product performance. The density of thin film influences e.g. the mechanical properties such as mechanical stability and stress, diffusion and barrier behavior, as well as optical quantities such as the refractive index. Roughness of surfaces and interfaces affects the adhesion of layers and optical scattering and losses. In addition, the surface roughness determines the tribological behavior. Film thicknesses are most important for the optical properties of the coatings. Most optical multi layer systems consist of $\lambda/2$ or $\lambda/4$ designs, which creates very unique optical features.

Modern GIXR equipment is necessary to obtain the required high accuracy of the experimental data. Different experimental setups are commercially available from a few suppliers. Also, different software is in use for simulation of the experimental data.

Experimental reflectivity curves need to be simulated using software when more than one layer is present on a substrate. The two main obvious sources of errors are:

- the shape of the experimental curve, due to a nonrigorous experimental setup,
- the theoretical parameters used in the simulation software.

This paper describes a GIXA Round Robin test carried out by three industrial laboratories. The objective of the work was to compare the influence of both the experimental setup and the simulation software on the results from the same set of samples. The three laboratories obtained GIXA data and used their own simulation software on their own

Received 24 October 2003.

data to determine the density and the film thickness. Each laboratory then used their simulation software on measured data received from one of the other two laboratories. A good agreement in the analyzed film parameters was obtained.

2. Experimental details

At grazing incidence all X-ray techniques become surface sensitive. Far below the angle of total reflection the X-rays penetrate only 2 to 7 nm into condensed matter. It turns out that GIXA is the right technique to match the measurement demands for thin layers on glass surfaces and their interfaces [1 and 2]. GIXR is based on the reflection of X-rays by flat surfaces. This reflection follows the classical optical principles of refraction and reflection with optical indices related to the wavelength used and to the medium's properties. X-rays are refracted according to Snell's law when they cross the interface of two media. In the hard X-ray range the index of refraction n is a complex number with a real part slightly smaller than 1 [3]. It can be written as $n = 1-\delta+i\beta$ (δ and β are positive and of the order 10^{-5} to 10^{-6}). The absorptive correction $\beta = \mu\lambda/(4\pi)$ is proportional to the coefficient of linear absorption μ and the photon wavelength λ. The dispersive correction δ is proportional to λ^2, to the mass density ρ and the real part $(Z+f')$ of the atomic form factor. Since n is smaller than one (1-δ), the beam is refracted away from the surface normal when it enters into the matter. Therefore, there exists a critical angle θ_{1c} for the incident beam at which the angle of the refracted beam $\theta_2 = 0$.=Below θ_{1c} the beam is totally reflected and so the absorption can be neglected – this occurs at $\theta_{1c} \cong \sqrt{2\,\delta_2}$. In the hard X-ray range this angle is below 0.5° for most materials. The determination of the critical angle gives the mass density of the reflecting medium.

In reality, however, θ_{1c} cannot be determined in a simple way from the reflectivity because the drop in reflectivity at the critical angle is smeared out by absorption and by surface roughness. The latter is taken into account by an exponential Debye Waller type factor to the Fresnel reflectivity derived from the model of Névot and Croce [4]. For more details upon X-ray reflectivity see [1, 5 and 6].

2.1 Instrument parameters

Table 1 shows the experimental instrument parameters used by the three laboratories, labeled as Lab A, Lab B and Lab C. For simple comparisons, the most relevant experimental data are summarized.

2.2 Instrument operational setups

The measurements in Lab A are performed by a standard Philips X'Pert materials research diffractometer (MRD) with PW1830 generator and optically encoded PW3020 goniometer (step size 0.0001° in θ). The X-ray source is a sealed tube with copper anode and long fine focus of optical height 40 µm. The programmable divergence slit (PDS) at the incident beam side produces a beam width of less than 0.04° in 2 θ. This allows an accurate calibration of the 2 θ zero position (direct beam) and an accurate adjustment of the sample with respect to the incident beam. On the diffracted beam side a programmable receiving slit (PRS) and a programmable anti-scatter slit (PASS) are used. They are set into coupled mode – both have the same fixed opening of 100 µm. An additional curved graphite monochromator in front of the detector (gas proportional counter) limits the detected wavelength range and Soller slits (0.04°) on both sides limit the axial divergence. The direct beam intensity at 45 kV/40 mA reaches $2 \cdot 10^7$ cps. Since the dynamic range of the X-ray detector is limited to $5 \cdot 10^5$ cps, an automatic attenuator (Ni-foil, factor 120) is used at high intensities, which increases the dynamic range in the measurement over 7 to 8 decades. The underground counting rate in this setup is 0.2 to 0.5 cps. The sample stage (open Eulerian cradle) is motorized and allows the adjustment of the sample in the direct beam with an accuracy in height of 1 µm and a tilt angle of 0.01°. The precise adjustment of the incident and reflected beam with an accuracy of better than 1 arc sec is done just below the critical angle by rotating the sample with fixed source and detector, as in the "rocking curve experiment".

Due to some production processes the shape of glass surfaces is not perfectly flat but slightly bent or undulated. These surface shapes may cause problems with the alignment of the sample and cause changes in the intensity near the critical angle in a reflectivity measurement. For this reason a beam knife a few µm above the sample surface is used to reduce the effective reflecting area of the sample. It improves the shape of the "plateau" in reflectivity curves below the critical angle and results in an accurate detection of the critical angle.

The measurements in Lab B are performed by a standard Siemens D5000 diffractometer with a step by step goniometer (step size 0.005° in 2 θ). The X-ray source is a sealed tube with copper anode and long fine focus. All the slits are fixed with the following dimensions : divergence slit = 0.05 mm, anti-scatter slit = 0.2 mm, resolution slit = 0.05 mm. An additional curved graphite monochromator in front of the detector (scintillator) limits the detected wavelength range and Soller slits on both sides limit the axial divergence. The direct beam intensity at 40 kV/30 mA reaches $\approx 7 \cdot 10^4$ cps with a copper attenuator which reduces the intensity by a factor of $\approx$ 60). Since the dynamic range of the X-ray detector is limited to $\approx 8 \cdot 10^4$ cps, this attenuator is necessary for high intensities (at low angle) to be sure to stay in the linearity domain of the detector but is not used at angles higher than about 1°. The dynamic range in the measurement is typically 6 to 7 decades. The sample stage (classical system with the possibility to move the sample along the Z axis and to adjust the tilt angle with two screws) allows the adjustment of the sample in the direct beam with an accuracy in height (Z axis) of a few microns. As for Lab A, the adjustment of the incident beam is obtained through a "rocking curve experiment" and a knife may be used during the acquisitions for the same reasons as given in Lab A, but has not been used in this case.

The measurements in Lab C performed by a standard Philips X'Pert materials research diffractometer (MRD) with a similar specification to that of Lab A. i.e. programmable divergence slit, programmable receiving and anti-scatter slits, curved graphite monochromator. The direct beam intensity at 45 kV/40 mA reaches $2 \cdot 10^7$ cps. Since the dy-

Table 1. Experimental parameters of instruments used in the three laboratories

experimental parameter	laboratory		
	A	B	C
X-ray source	CuK_α, LFF 45 kV, 40 mA	CuK_α, LFF 40 kV, 30 mA	CuK_α, LFF 30 kV, 10 mA
Soller slit	0.04°	0.04°	0.04°
divergence slit	1/50°	50 µm	1/32°
sample stage	open Eulerian cradle	classical system	open Eulerian cradle
sample adjustment	height: ± 1 µm tilt: ± 0.01° θ, 2θ: ± 0.001°	height: ± 1 µm tilt: ± 0.01° θ, 2θ: ± 0.001°	height: ± 1 µm tilt: ± 0.01° θ, 2θ: ± 0.001°
beam cut knife	yes (only used for nonflat samples)	yes (not used here)	no (not required for flat samples)
anti-scatter slit	100 µm	200 µm	1/32°
receiving slit	100 µm	50 µm	100 µm
secondary monochromator	curved graphite	curved graphite	curved graphite
detector	gas proportional counter	scintillator (NaJ:Tl)	gas proportional counter
dynamic range	7 to 8 decades	6 to 7 decades	4 to 5 decades
maximum counts	$18 \cdot 10^6$ cps	$3 \cdot 10^6$ cps	$1.15 \cdot 10^6$ cps
background	0.2 to 0.5 cps	1 cps	14 cps
starting angle (2θ)	0°	0°	0.1°
step size (2θ)	0.004°	0.005°	0.01°
end angle (2θ)	8°	usually 8°	3°
data points	2001	depends on scan range	290
time per step	12 s	usually 10 to 15 s	5 s
scan mode	continuous	step scan	continuous

namic range of the X-ray detector is limited to $5 \cdot 10^5$ cps, GIXA measurements are carried out at 30 kV/10 mA. The lower power settings remove the effects of detector saturation and the shape of the "plateau" at low 2θ angle is much improved. A measurement dynamic range of 4 to 5 decades is produced and the background count in this setup is approximately 14 cps. The sample alignment is the same as in Lab A.

Due to some production processes, the shape of glass surfaces is not perfectly flat but slightly bent or undulated again. For nonflat/curved substrates the standard 10 mm incident beam mask is replaced with a 5 mm mask to reduce beam divergence and improve the shape of the "plateau" below the critical angle. This results in an improved detection of the critical angle, however, the overall incident beam X-ray intensity is reduced.

2.3 Simulation software

The information which can be extracted from the reflectivity curve (X-ray intensity versus angle of incidence) includes:

- the density ρ of the coating layers and of the substrate,
- the thickness d of the layers,
- the surface and interface roughness σ (rms value).

In Lab A, the information from the experimental data is extracted with the Philips GIXA software [7]. It is based on the transfer matrix method [8] and uses the simplex algorithm in combination with simulated thermal annealing [9]. It requires user inputs of estimates of instrumental resolution and sample parameters (number of layers, starting values). Starting values of the layer thickness are obtained by a Fourier transformation of the experimental curve. The data analysis needs values for the dispersive correction to the atomic scattering factor $f'(E)$. These data were taken from calculation [10 and 11].

Table 2. Film system and producer of investigated samples

sample no.	film system	producer
1	28 nm TiN/12 nm Inox/glass	Saint-Gobain
2	25 nm ZnO/14 nm SnO_2/glass	Saint-Gobain
3	26 nm ITO/glass	Pilkington
4	5 nm SiO_2/63 nm TiO_2/31 nm SiO_2/glass	SCHOTT
5	70 nm MgF_2/50 nm MgO/glass	SCHOTT

In Lab B, the simulation software Refsim (Bruker software) is used, which can extract density (also the parameter δ), thickness and roughness for each layer. The software cannot simulate the terms δ and β. Fast Fourier transform (FFT) is available to estimate thickness.

In Lab C, the information from the experimental data is extracted with the Philips WIN-GIXA software = the Windows version of the software used by Lab A. The simulation produces estimates of thickness, density, surface roughness and interface roughness for each layer.

2.4 Sample descriptions

Five samples with different coatings (single and multi layers) on soda-lime-silica glass substrates from the three companies were used for the Round Robin test. Each film's materials and film thickness estimated by the producer are given in table 2.

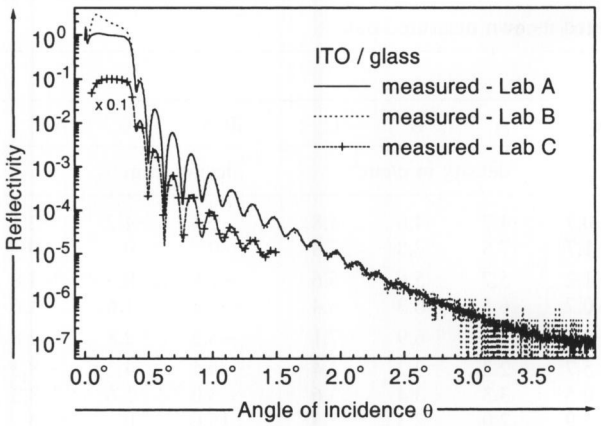

Figure 1. Experimental reflectivity curves for ITO coated glass (sample 3) measured in Labs A, B and C. The graph of Lab C is shifted for better representation.

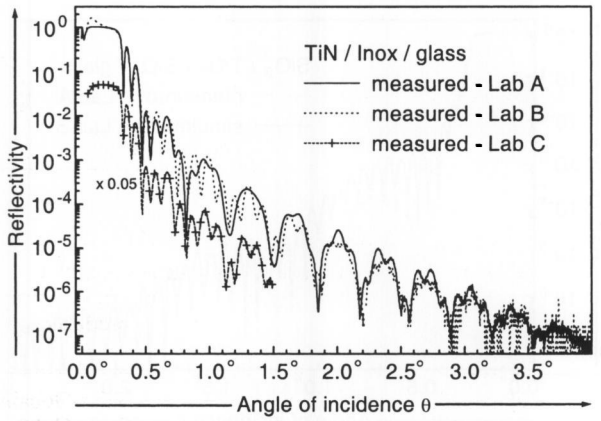

Figure 2. Experimental reflectivity curves for TiN/Inox on glass (sample 1) measured in Labs A, B and C. The graph of Lab C is shifted.

3. Results

Typical experimental results obtained from the five samples, analyzed in the three laboratories, are presented. In addition, numerical data on film thickness and film density, obtained from simulation, are evaluated. These numerical data are compared and they are examined by means of the Youden plots.

3.1 Graphical results

Figure 1 shows the experimental results of a single layer on glass, ITO/glass (sample 3), measured in the different laboratories. For clearer representation the data of Lab C are shifted. The three reflectivity curves are very similar. This demonstrates that the different instrument types and data acquisition parameters produced similar experimental data. In the plateau region (high reflectivity, low angle) a good agreement is observed between Labs A and C. Small deviations are observed for Lab B. In the low reflectivity region (high angle) the data variability is much lower for Lab A compared with Lab B. Data for Lab C are not shown for the low reflectivity range. There is, in general, good agreement of the experimental data from the different laboratories obtained with different instruments. This indicates that the technique is well established but also that the investigated samples seem to be fairly independent of cleaning and storage in the environment.

The experimental reflectivity curves of the two-layer system TiN/Inox[1]/glass (sample 1) are summarized in figure 2. The obtained data are in both the low and the high angle regions nearly identical for the different laboratories. Again, Labs A and C produced a well defined flat plateau region, which is difficult to recognize for Lab B. More oscillations are present in the data from Labs B and C, particularly between 1.0° and 1.5°. However, compared to Lab A the oscillations are less pronounced for Labs B and C in this region. The small frequency shift between Labs A and B indicates a change in the sample density. Table 3 shows that among the three laboratories, Lab B produced the lowest density for the TiN layer. This suggests a modified surface layer.

In figures 3a and b measured reflectivity curves are shown for sample 5 (MgF_2/MgO/glass). These are compared with simulated reflectivity curves. The results are shown from Labs A and C, i.e. the experiments and the mathematical simulation are done in the same laboratory. Overall, there is good agreement between the experimental curves and the simulated curves, i.e. the agreement is high when both Labs A and C simulated their own data. Both laboratories used theoretical models, which consist of two homogeneous layers with well defined interfaces. The good agreement between theoretical and experimental data shows that the theoretical model used is an accurate description of the coating stack (reality). The numerical data for film thickness and density are given in table 3.

The reflectivity curve measured in Lab A on a three-layer system consisting of SiO_2/TiO_2/SiO_2/glass (sample 4) is shown in figure 4. The simulation was carried out in Lab B. Although the simulated curve is in a good agreement with the measured curve at low angle of incidence, there is a marked shift in the positions of the oscillations at higher angles. This demonstrates that the simulated curve produced by the software has a different 'resolution' from that of the experimental data. The software works with an ideal resolution and not with that derived from the instrumental parameters. In addition, the simulation does not produce an accurate background.

Figures 5a and b show measured and simulated curves obtained on a double layer system ZnO/SnO_2/glass (sample 2). The experimental data are obtained in Lab B while the two simulated curves are from Labs A and C. The experimental data and the simulation fit very well and are independent of the laboratory. This comparison demonstrates the use of effective software in both laboratories. The simulated background between an angle of incidence of 2.2° and 2.6° is slightly higher than the measured background. This effect is due to the simulation software failing to obtain a satisfactory average background when count rates are very low.

Figures 6a and b compare the measured reflectivity curves with simulation curves. The data of sample 1 (TiN/Inox/glass)[2] are measured and simulated in the same labor-

[1] Inox = stainless steel.

Table 3. Comparison of thickness and density; each laboratory simulated its own measured data

sample no.	film composition	laboratory											
		A	B	C	B/A	B/C	A/C	A	B	C	B/A	B/C	A/C
		thickness in nm			deviation in %			density in g/cm³			deviation in %		
1	TiN	29.0	27.7	29.2	−4.5	−5.1	−0.7	4.7	4.6	4.8	−2.1	−4.2	−2.1
	Inox	12.3	12.3	12.1	0	1.7	1.7	7.8	7.8	7.8	0	0	0
2	ZnO	23.8	24.6	24.1	3.4	2.1	−1.2	5.7	5.6	5.6	−1.8	0	1.8
	SnO_2	13.8	13.8	13.7	0	0.7	0.7	6.5	6.3	6.4	−3.1	−1.6	1.6
3	ITO	26.2	26.3	26.3	0.4	0	−0.4	7.3	6.9	7.1	−5.5	−2.8	2.8
	SiO_2	5.6	5.6	5.3	0	5.7	5.7	2.2	2.3	2.4	4.5	−4.2	−8.3
4	TiO_2	62.9	63.1	63.2	0.3	−0.2	−0.5	3.3	3.4	3.6	3.0	−5.6	−8.3
	SiO_2	30.5	31.9	32.4	4.6	−1.5	−5.9	2.0	2.3	2.3	15.0	0	−13
5	MgF_2	70.2	70.1	70.4	−0.1	−0.4	−0.3	2.8	2.9	3.0	3.6	−3.3	−6.7
	MgO	49.7	49.2	49.8	−1.0	−1.2	−0.2	3.4	3.4	3.5	0	−2.9	−2.9

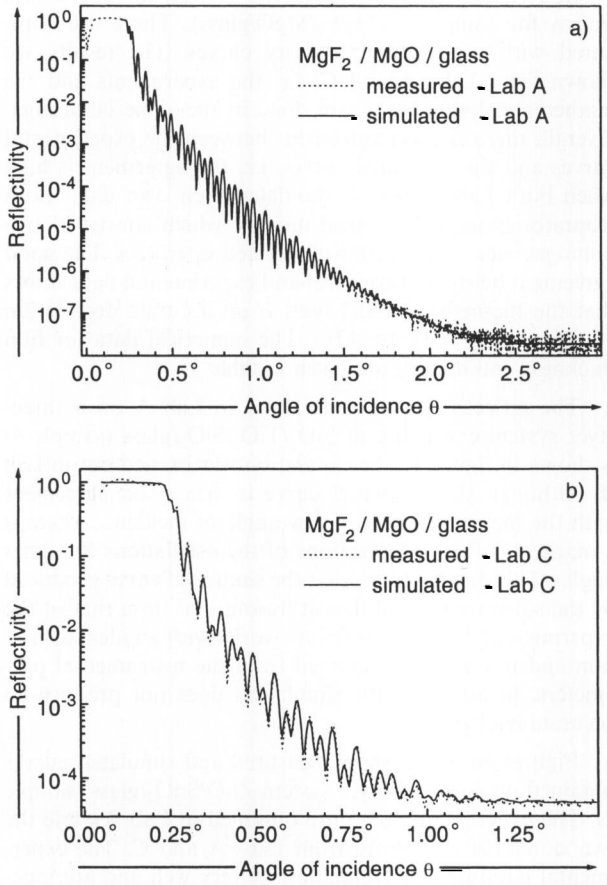

Figure 3a and b. Comparison of experimental reflectivity curves and high accuracy simulation for MgF_2/MgO on glass (sample 5) measured in a) Lab A and b) Lab C. Both laboratories simulated their own data.

atory. One data set demonstrates the effect when the software resolution is not in agreement with the obtained experimental data (Lab B). For the second data set there is a very good agreement between measured data and simulation in the low angle range (Lab C).

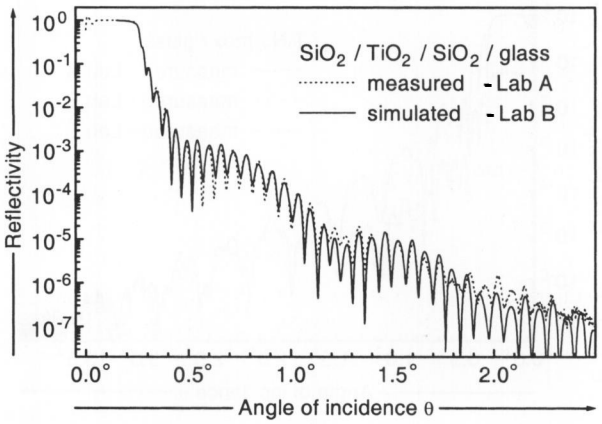

Figure 4. Comparison of experimental reflectivity curves obtained for $SiO_2/TiO_2/SiO_2$ on glass (sample 4) measured in Lab A with simulation of Lab B.

3.2 Numerical results

By the simulation of the experimental curves depicted in the previous section, numerical data for film thickness, density and surface and interface roughness may be obtained in principle. The analyzed numerical results on film thickness and film densities of the five samples are summarized in tables 3, 4, 5 and 6. Data on roughness are not shown.

Table 3 shows data from the simulation of 'own' experimental data, i.e. each laboratory measured and simulated its own data. In addition, the deviations between the three laboratories are given in percentage. Table 4 presents the numerical results of the simulations of Lab C of the experimental curves from Labs B and C. Thicknesses and densities of the different films are compared and the deviations are given. Table 5 is similar to table 4 but contains data from the simulation of Lab A of its own curves and of the measured results of Lab B. Table 6 shows the data of the simulation of Lab B of the experimental curves of Lab A.

The upper part of table 3 contains the obtained layer thickness of the five samples. In general, the film thicknesses are fairly low, i.e. in the range of 5 to 70 nm. This thickness

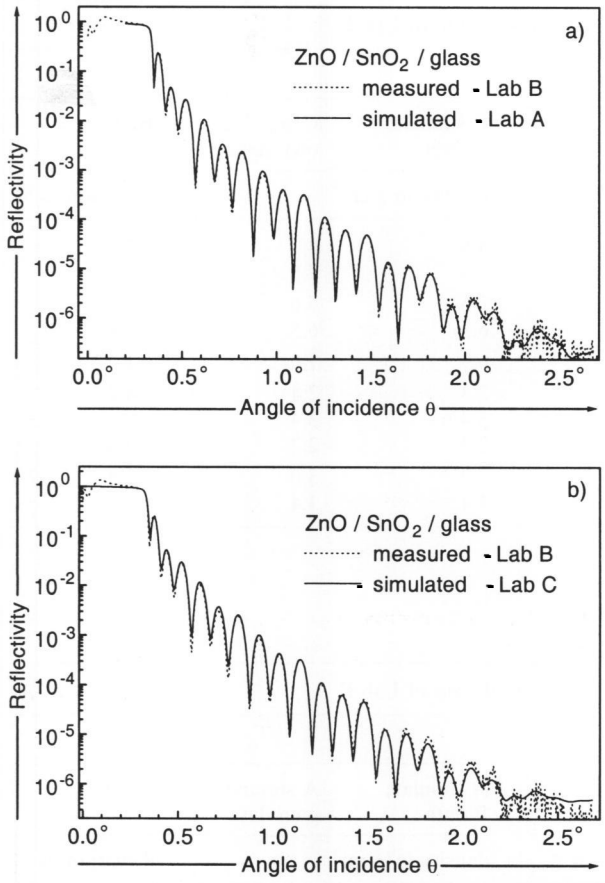

Figures 5a and b. Comparison of experimental and simulated reflectivity curves from ZnO/SnO_2/glass (sample 2). The measured data are from Lab B and the simulation from a) Lab A and b) Lab C.

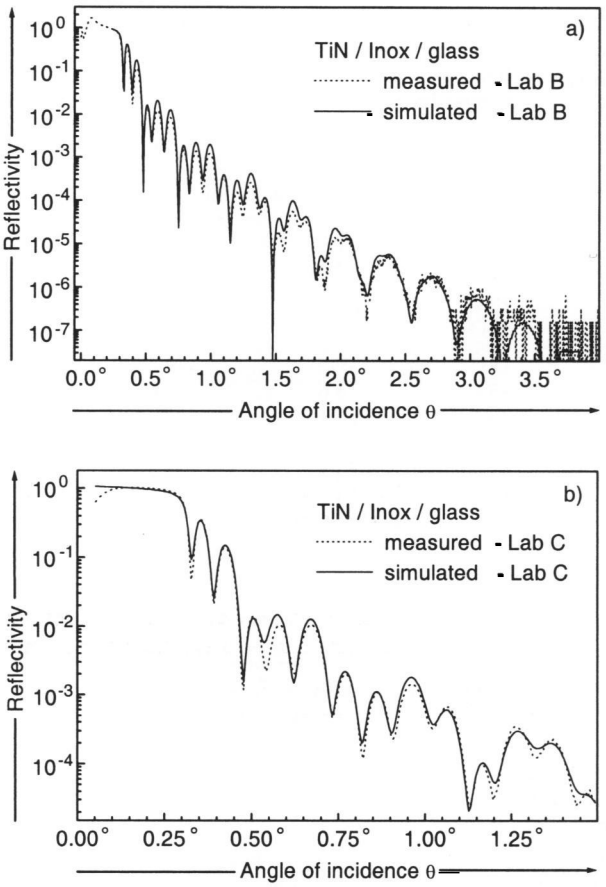

Figures 6a and b. Measured and simulated reflectivity curves of TiN/Inox on glass (sample 1); a) measurement curves and simulation obtained by Lab B, b) data from Lab C.

range is difficult to determine by other techniques with a high accuracy. The mean deviations for the film thickness between Labs A and B are: 0.3 ± 2.4 %, between Labs B and C: 0.2 ± 2.8 %, and between Labs A and C: − 0.1 ± 2.8 %. The high accuracy is demonstrated on the single-layer system (sample 3) where the deviation between the laboratories is smaller than 0.5 %. Also, for the double-layer system (sample 5) with the relative high film thickness, low deviations are observed. For the second two-film system (sample 1) the obtained data show a higher deviation. The largest deviations between the laboratories are found for sample 4, which is a more complicated three-layer system. In particular, the SiO_2 thickness shows a relatively high deviation.

The film densities of the different films show an overall good agreement (table 3). The mean deviation for the density between Labs A and B is: 1.4 ± 5.7 %, between Labs B and C: −2.5 ± 2.0 %, and between Labs A and C: −3.5 ± 5.3 %. Again the most complicated film system (sample 4) shows the largest deviation in particular for the SiO_2 layers. It should be noted that the density values of 2.3 and 2.4 g/cm^3 for sample 3 appear too high because the layer is produced by dip coating. It is generally regarded that a dip coated SiO_2 layer has a lower density than quartz SiO_2 (2.4 g/cm^3). Therefore, the density values of Labs B and C are probably too high.

Table 4 summarizes the data on thickness and density. The simulations were carried out by Lab C on the experimental data obtained by Lab B. Comparisons are made with the Lab C simulations of its own data. The film thicknesses demonstrate the high accuracy of the experimental technique. The mean thickness variation between the two laboratories is 0.02 ± 0.7 %. The deviations between the two laboratories for the density are higher. However, it should be mentioned that the simulations of Lab C of its own data were similar to those obtained when Lab C simulated the data of Lab B. In both cases higher than expected density values were obtained in particular for sample 4 for the SiO_2 layer. On the basis of this data it can be surmised that the type of instrument used and the acquisition procedure are less important than the experience and the background of the operator. The mean density variations are −0.7 ± 2.7 %.

Table 5 shows the results of the simulation that Lab A carried out on the experimental data of Lab B. For comparison, Lab A's own data are shown. Again, the deviations in both film thickness and density are relatively small. The mean thickness variation is −0.2 ± 2.2 % between the simulated data of Lab A and the data of Lab B. This mean variation is larger than that between Labs C and B. The mean density variation is −0.5 ± 2.0 %.

The same procedure as in tables 4 and 5 is shown in table 6. Numbers are given for the simulation carried out by Lab B on the data of Lab A. Also shown are Lab B's

Table 4. Comparison of thickness and density; Lab C simulated the experimental data of Lab B

sample no.	film composition	laboratory					
		C simulate B data	C simulate own data	B / C	C simulate B data	C simulate own data	B / C
		thickness in nm		deviation in %	density in g/cm^3		deviation in %
1	TiN	27.7	27.9	−0.7	4.6	4.7	−2.1
	Inox	12.3	12.2	0.8	7.8	7.6	2.6
2	ZnO	24.6	24.6	0	5.6	5.6	0
	SnO_2	13.8	13.7	0.7	6.3	6.5	−3.1
3	ITO	26.3	26.3	0	6.9	7.0	−1.4
4	SiO_2	5.6	5.6	0	2.3	2.4	−4.2
	TiO_2	63.1	62.9	0.3	3.4	3.4	0
	SiO_2	31.9	32.3	−1.2	2.3	2.2	4.5
5	MgF_2	70.1	69.9	0.3	2.9	3.0	−3.3
	MgO	49.2	49.4	−0.4	3.4	3.4	0

Table 5. Comparison of thickness and density; Lab A simulated the experimental data of Lab B

sample no.	film composition	laboratory					
		A simulate B data	A simulate own data	B / A	A simulate B data	A simulate own data	B / A
		thickness in nm		deviation in %	density in g/cm^3		deviation in %
1	TiN	27.8	29.0	−4.1	4.7	4.7	0
	Inox	12.2	12.3	−0.8	7.5	7.8	−3.8
2	ZnO	24.6	23.8	3.4	5.6	5.7	−1.8
	SnO_2	13.7	13.8	−0.7	6.3	6.5	−3.0
3	ITO	26.1	26.2	−0.4	7.3	7.3	0
4	SiO_2	5.5	5.6	−1.8	2.2	2.2	0
	TiO_2	63.0	62.9	0.2	3.3	3.3	0
	SiO_2	31.4	30.5	3.0	2.0	2.0	0
5	MgF_2	70.0	70.2	−0.3	2.9	2.8	3.6
	MgO	49.5	49.7	−0.4	3.4	3.4	0

Table 6. Comparison of thickness and density; Lab B simulated the experimental data of Lab A

sample no.	film composition	laboratory					
		B simulate A data	B simulate own data	A / B	B simulate A data	B simulate own data	A / B
		thickness in nm		deviation in %	density in g/cm^3		deviation in %
1	TiN	27.5	27.7	−0.7	4.6	4.6	0
	Inox	12.3	12.3	0	7.8	7.8	0
2	ZnO	24.0	24.6	−0.8	5.6	5.6	0
	SnO_2	13.8	13.8	0	6.3	6.3	0
3	ITO	26.0	26.3	−1.1	7.0	6.9	1.4
4	SiO_2	5.6	5.6	0	2.3	2.3	0
	TiO_2	63.1	63.1	0	3.4	3.4	0
	SiO_2	31.9	31.9	0	2.3	2.3	0
5	MgF_2	70.3	70.1	0.3	2.8	2.9	−3.4
	MgO	49.6	49.2	0.8	3.4	3.4	0

Table 7. Comparison of the film thickness of sample no. 1, 2 and 5

sample no.	film composition	laboratory			mean value in nm
		A	B	C	
		mean value in %			
1	TiN	101.3	96.8	102.0	28.63
	Inox	100.6	100.6	98.9	12.23
2	ZnO	98.5	101.8	99.7	24.17
	SnO_2	100.2	100.2	99.5	13.77
5	MgF_2	100.0	99.8	100.2	70.23
	MgO	100.3	99.3	100.5	49.57

Table 8. Comparison of the film density of sample no. 1, 2 and 5

sample no.	film composition	laboratory			mean value in g/cm³
		A	B	C	
		mean value in %			
1	TiN	100.0	97.9	102.1	4.70
	Inox	100.0	100.0	100.0	7.80
2	ZnO	101.2	99.5	99.5	5.63
	SnO_2	101.6	98.4	100.0	6.40
5	MgF_2	96.6	100.0	103.4	2.90
	MgO	99.1	99.1	102.0	3.43

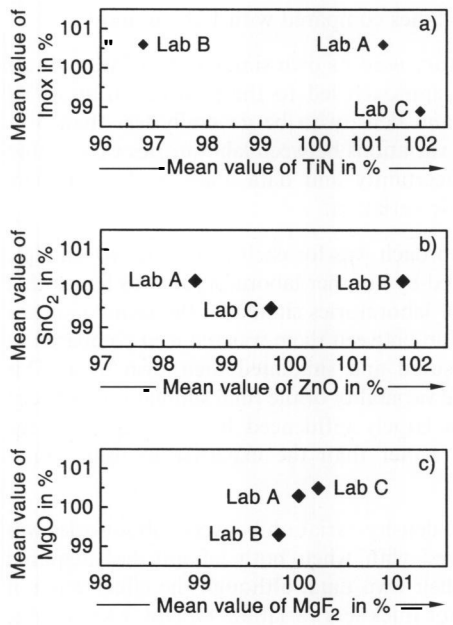

Figures 7a to c. Youden plots for comparison of the film thickness (expressed as percentage of the mean value) of sample a) no. 1, b) no. 2, and c) no. 5.

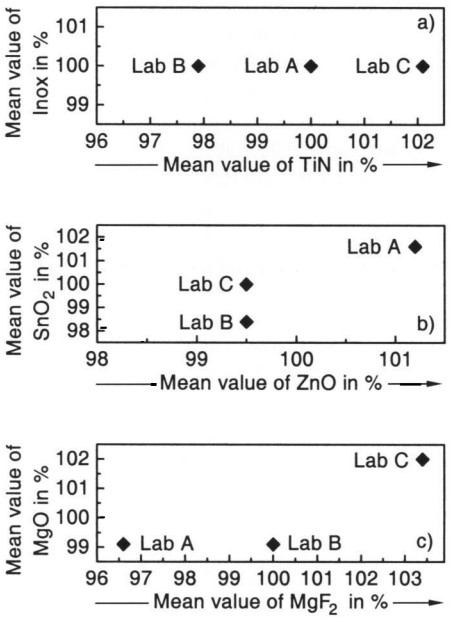

Figures 8a to c. Youden plots for comparison of the film density (expressed as percentage of the mean value) of sample a) no. 1, b) no. 2, and c) no. 5.

simulated data of its own experimental results. For both thicknesses and densities, the deviations between the data of Labs B and A are very small. The mean thickness variation between the two laboratories is $0.2 \pm 0.6\,\%$ and the mean density variation is $-0.2 \pm 1.2\,\%$.

3.3 Statistical analysis using Youden plots

The film thickness and density values obtained from Labs A, B and C (simulation of their own data) are examined by means of Youden plots. Each measurement value (thickness or density) is expressed as a percentage of the mean value of the measurement variable from the three laboratories (tables 7 and 8). The approach graphically shows any systematic variation between laboratories.

Figures 7a to c and 8a to c show typical examples of the types of plots that were obtained. Figures 7a to c show thickness values, expressed as a percentage of the mean value, for samples 1, 2 and 5. Figures 8a to c present the respective density values. Analysis of these figures clearly shows that there is no systematic variation in thickness and density values between Labs A, B and C. This indicates that no systematic bias exists between the laboratories in terms of both data acquisition and simulation of experimental results.

4. Discussion

4.1 Differences in experimental data

The reflectivity curves produced by the three laboratories are similar, which indicates that different instrument types and data acquisition parameters produced similar measured data. However, differences in measured data are discernable, notably in the low angle (high reflectivity) or plateau region, in both the periods of reflectivity oscillation and in the background level/variation at high angle.

For sample 1 (TiN/Inox/glass), both Labs A and C produced a flat plateau region compared with Lab B. It is suggested that this is due to the use of a beam cut-knife in Lab A and low voltage/current settings in Lab C – both these having the effect of reducing detector saturation at high

count rates. The improved counting statistics of the Lab A data in the low reflectivity region is probably due to a longer counting time per measurement step. The increased frequency of reflectivity oscillation between 1 and 2 degrees for Lab B indicates an increased thickness for one of the layers. This suggests the formation of a modified surface layer in the storage environment between Lab A and Lab B measurements.

Lab B analyzed this sample several months after Lab A. It can be hypothesized that the TiN layer had become partially oxidized over this time period, resulting in a more porous and less dense TiN at the surface – a modified surface layer. Indeed, table 3 shows that of the three laboratories, Lab B produced the lowest density for the TiN layer.

Sample 2 (ZnO/SnO_2/glass) shows a small shift in reflectivity oscillation between Labs A and B. Again, a thin surface film may have been created during sample storage. Sample 3 (ITO / glass) produced very similar data from the three companies. As for sample 1, Lab A and C had a flat plateau region compared with Lab B, and Lab A had the best counting statistics. These differences can again be explained by the use of a beam cut knife (Lab A), lower power settings (Lab C) and a higher counting times / measurement step (Lab A).

Samples 4 ($SiO_2/TiO_2/SiO_2$/glass) and 5 (MgF_2/MgO/glass) both produced similar reflectivity curves for the three laboratories. Density values of 2.3 and 2.4 for the SiO_2 layers are a little high and against expectations since the density of silica layers in coatings is generally believed to be much lower than that of naturally occurring silica.

4.2 Differences in simulated data

The first situation to consider is when each laboratory measured and simulated its own data. Reference should be made to table 3. The relative variations of both thickness and density measurements are in most cases less than 5 %. Statistically, the variations between the three laboratories are the same, within experimental uncertainty.

The second situation is when each laboratory simulated the data measured by another laboratory. Reference should be made to tables 4, 5 and 6. In all three cases, both the mean and the standard deviation between 'Lab X' and 'Lab Y' was reduced compared with when these laboratories simulated their own data. When two laboratories simulated the same data, the thickness variation between them is less compared to when they measured and simulated their own data. This is an important observation since it indicates that the variability of the final simulations between laboratories depends on the quality of the measured data, rather than the expertise in using simulation software. Similarly, the density variation between laboratories is reduced compared with when both laboratories acquired and simulated their own data, although the effect is not as great as that for thickness variation.

Finally, the Youden plots show that there is no systematic bias between laboratories for thickness (figures 7a to c) nor for density (figures 8a to c).

5. Conclusion

The three laboratories each obtained GIXA reflectivity curves from five single and multilayer coatings. Although the measured data from the three laboratories were similar, some differences were evident. The largest was in the plateau region at low 2 θ angle. Labs A and C produced a flat plateau compared with Lab B. This is believed to be due to the use of a beam knife by Lab A, which reduces the 'interference reflections' from nonflat surfaces and also reduces X-ray intensity at the detector. Lab C did not use a beam knife but X-ray intensity was reduced throughout the whole measurement by using lower kV/mA settings compared with Labs A and B. Lab A was able to achieve the best data statistics in the low reflectivity region by using longer counting times compared with Labs B and C.

Each laboratory used its own simulation software on its own data. This approach led to the relative variations of both thickness and density to be generally less than 5 %. Statistically, the variations between laboratories were within experimental uncertainty and data analysis showed there was no systematic variation.

A second approach was for each laboratory to simulate the data measured by another laboratory. It was found that when any pair of laboratories simulated the same data, the thickness variation between them was reduced compared to when they measured and simulated their own data. This indicates that the variability of the final simulations between laboratories was largely influenced by the quality of the measured data, rather than the expertise in using simulation software.

Similarly, the density variation between laboratories was reduced compared with when both laboratories acquired and simulated their own data, although the effect was not as great as that for thickness variation. Operator knowledge and experience appears to have a greater influence on density measurement than does the instrument type/setup and the data acquisition procedure. Overall, the operators in Labs A, B and C appear to have similar levels of proficiency in both data acquisition and the use of simulation software.

6. References

[1] Lengeler, B.; Campagna, M.; Rosei, K. (eds.): X-ray absorption and reflection in the hard X-ray range. Photoemission and absorption spectroscopy of solids and interfaces with synchrotron radiation. Amsterdam: North Holland, 1990.

[2] Zabel, H.; Robinson, K. (eds.): Surface X-ray and neutron scattering. Berlin et al.: Springer, 1992.

[3] James, R. W.: The optical principles of the diffraction of X-rays. Ithaca, NY: Cornell University Press, 1965. Chapter 4.

[4] Névot, L.; Croce, P.: Caractérisation des surfaces par réflexion rasante de rayons X. Application à l'étude du polissage de quelques verres silicates. Rev. Phys. Appl. **15** (1980) no. 3, pp. 761–779.

[5] Lengeler, B.; Hüppauff, M.: Surface analysis by means of reflection, fluorescence and diffuse scattering of hard X-ray. Fresenius J. Anal. Chem. **346** (1993) pp. 155–161.

[6] Lengeler, B.; Hasnain, S.S. (ed.): X-ray absorption fine structure. Chichester: Horwood (Ellis), 1991.

[7] Program "GIXA", PHILIPS Analytical X-ray. Almelo (Netherlands) 1992.

[8] Parratt, L. G.: Surface studies of solids by total reflection of X-rays. Phys. Rev. **95** (1954) pp. 359–369.
[9] Press, W. H.; Teukolsky, S. A.: Simulated annealing optimization over continuous spaces. Comput. Phys. **4** (1991) pp. 426–429.
[10] Kissel, L.; Pratt, R. H.: Corrections to tabulated anomalous scattering factors. Acta Cryst. **A46** (1990) pp. 170–175.
[11] Cromer, D. T.: Program "FPRIME" (Program to interpolate cross sections and compute anomalous scattering factors). Los Alamos, NM: 1992. Internet document: http://www.ccp14.ac.uk/ccp/ccp14/ftp-mirror/ansto/pub/physics/neutron/Anomalous/Fprime.for, or: http://www.uni.aps.anl.gov/cgi-bin/fprime.

E204P002

Contact:

Dr. O. Anderson
SCHOTT GLAS
Hattenbergstraße 10
D-55122 Mainz
E-mail: Olaf.Anderson@schott.com